Supporting Information

Chiral Dicarbazole-Ditriarylamine Hole Transport Materials for Circularly Polarized Electroluminescence

Yuchang Wang,[#] Jiahao Xu,[#] Xiao Wang, Shujuan Liu, Yuxia Zhang,* Xinwen Zhang,* Yun Ma,* Qiang Zhao*

Table of Contents

1. Materials and Measurements

Unless otherwise stated, all starting materials and reagents were purchased from commercial suppliers and used without further purification. All solvents were purified before use. The solvents were carefully dried and distilled from appropriate drying agents prior to use. ^{1}H NMR (400 MHz) and ^{13}C NMR (100 MHz) spectra were recorded with deuterated solvent at 298 K by Bruker ACF400 spectrometer. Chemical shifts cite ppm relative to tetramethylsilane (TMS) (0.00 ppm), using the residual solvent peak as a reference standard (^{1}H NMR: $CDCl_3$ 7.26 ppm; ^{13}C NMR: $CDCl_3$ was 77.0 ppm). The UV-Vis absorption spectrum was determined by Shimazu UV-2600 UV-Vis absorption spectrometer. The emission spectrum was measured by Hitachi F-7000 fluorescence spectrophotometer. The fluorescence lifetime was determined by the Edinburgh FIS980 transient spectrometer. Thermogravimetric analysis (TGA) was performed on STA 449F3 simultaneous TG-DTA analyzer (Netzsch, Germany) with a heating rate of 10 °C/min from 25 °C to 600 °C under a nitrogen atmosphere. The glass transition temperature of the polymer was assessed using a DSC 823e differential scanning calorimeter (Mettler Toledo, Switzerland) under a nitrogen atmosphere. The sample was heated from 25 °C to 300 °C at a rate of 10 °C/min, held at 300 °C for 3 min, then cooled back to 25 °C, and this entire heating–cooling cycle was repeated twice.The cyclic voltammetry (CV) measurements were conducted on the CHI-600C electrochemical workstation in the traditional three-electrode system, where glass carbon electrode as the working electrode, Ag/AgCl electrode as the reference electrode, the platinum wire electrode as the auxiliary electrode, and the scan rate was 100 mV/s. Circular dichroism (CD) and circularly polarized luminescence/electroluminescence (CPL/CP-EL) spectra were measured by JASCO J-810 circular dichroism spectropolarimeter and JASCO CPL-300 spectrofluoropolarimeter, respectively.

2. OLEDs Fabrication and Measurement

All OLEDs were fabricated on pre-patterned ITO-coated glass substrates with a sheet resistance of 15 $\Omega\,sq^{-1}$. The organic compounds were deposited under vacuum (6 x 10^{-4} Pa) at a rate of 160℃-200℃ and 1-2 A s^{-1}.The phosphor and host material were co-evaporated from two separate sources to form the emitting layer. The cathode, consisting of Liq/Al, was deposited by first evaporating Liq at a rate of 1 Å s^{-1}, followed by the evaporation of Al metal at a rate of 2-4 Å s^{-1}. The characteristic curves (*J-V*) of the devices were measured with a computer controlled KEITHLEY 2602 source meter with a calibrated silicon diode in air without device encapsulation. Based on the uncorrected EL spectra were calculated using a test program of the Spectra scan PR650 spectrophotometer. The characteristic curves of the devices were measured using a computer-controlled KEITHLEY 2602 source meter with a calibrated silicon diode, under ambient conditions without device encapsulation. The external quantum efficiency (*EQE*) of the EL devices was determined using photon energy measurements obtained from the photodiode.

3. Synthesis of *R/S*-TPA:

R/S-1,1′-Binaphthyl-2,2′-diamine (2.0 g, 7.0 mmol), bromobenzene (2.4 g, 15.4 mmol), tri-tert-butylphosphine tetrafluoroborate (406 mg, 1.4 mmol), and sodium tert-butoxide (1.48 g, 15.4 mmol) were dissolved in toluene (25 mL). The solution was then charged with $Pd_2(dba)_3$ (320 mg, 0.35 mmol) under

a nitrogen atmosphere and heated at 110 °C for 24 h. The reaction progress was monitored by thin-layer chromatography (TLC). After completion, the mixture was cooled to room temperature, filtered to remove inorganic residues, and concentrated under reduced pressure. The crude product was purified by flash column chromatography on silica gel (petroleum ether/dichloromethane, 3:1, v/v), affording *R/S*-TPA as a white solid (2.2 g, 73% yield). ^{1}H NMR (DMSO-*d6*, 400 MHz) δ (ppm): 7.93 (d, *J* = 9.0 Hz, 2H), 7.87 (d, *J* = 7.8 Hz, 2H), 7.61 (d, *J* = 9.0 Hz, 2H), 7.32 - 7.22 (m, 2H), 7.21 - 7.09 (m, 6H), 7.03 - 6.93 (m, 6H), 6.82 - 6.76 (m, 2H), 6.73 (s, 2H). ^{13}C{^{1}H} NMR ($CDCl_3$, 100 MHz) δ (ppm): 142.0, 141.1, 139.7, 134.0, 131.4, 129.8, 129.8, 128.4, 128.2, 127.3, 125.8, 124.6, 124.0, 123.1, 120.2, 120.2, 119.7, 118.2, 117.4, 109.6.

4. Synthesis of *R/S*-CzTPA and *R/S*-BuCzTPA

R/S-TPA (1.0 g, 2.3 mmol), 9-(4-bromophenyl)-9H-carbazole (2.22 g, 6.9 mmol), tri-tert-butylphosphine tetrafluoroborate (133 mg, 0.46 mmol), and sodium tert-butoxide (420 mg, 5.0 mmol) were dissolved in toluene (15 mL) in the presence of $Pd_2(dba)_3$ (105 mg, 0.11 mmol) under a nitrogen atmosphere. The resulting mixture was stirred at 110 °C for 24 h. The progress of the reaction was monitored by thin-layer chromatography (TLC). Upon completion, the reaction mixture was cooled to room temperature, filtered to remove inorganic solids, and concentrated under reduced pressure. The crude residue was subsequently purified by flash column chromatography on silica gel (petroleum ether/dichloromethane, 3:1, v/v) to afford ***R/S*-CzTPA** as a white solid (1.60 g, 76% yield). ^{1}H NMR ($CDCl_3$, 400 MHz) δ (ppm): 7.99 (d, *J* = 8.0 Hz, 4H), 7.84 (d, *J* = 8.4 Hz, 2H), 7.68 (m, 4H), 7.41 - 6.99 (m, 14H), 6.98 - 6.41 (m, 22H). ^{13}C{^{1}H} NMR ($CDCl_3$, 100 MHz) δ (ppm): 144.1, 140.8, 134.1, 132.0, 131.5, 129.3, 128.6, 127.5, 126.9, 126.7, 125.6, 125.5, 125.2, 123.0, 120.1, 119.6, 110.0. HRMS (ESI): m/z Calculated for $C_{68}H_{46}N_4Na^+$ [M+Na^+]: 941.3615; Found 941.3576. ***R/S*-BuCzTPA** (white solid, 68% yield): ^{1}H NMR ($CDCl_3$, 400 MHz) δ (ppm): 8.06 (s, 4H), 7.92 (d, *J* = 8.4 Hz, 2H), 7.84 - 7.69 (m, 4H), 7.55 - 7.31 (m, 4H), 7.20 - 7.05 (m, 6H), 7.04 - 6.53 (m, 22H), 1.45 (s, 36H). ^{13}C{^{1}H} NMR ($CDCl_3$, 100 MHz) δ (ppm): 144.1, 142.4, 139.1, 134.1, 132.0, 131.5, 129.2, 128.6, 127.5, 126.9, 126.7, 126.5, 125.6, 123.2, 123.0, 116.0, 109.5, 34.7, 32.1. HRMS (ESI): m/z Calculated for $C_{84}H_{78}N_4Na^+$ [M+Na^+]: 1165.6119; Found 1165.6104.

5. TGA and DSC Curves

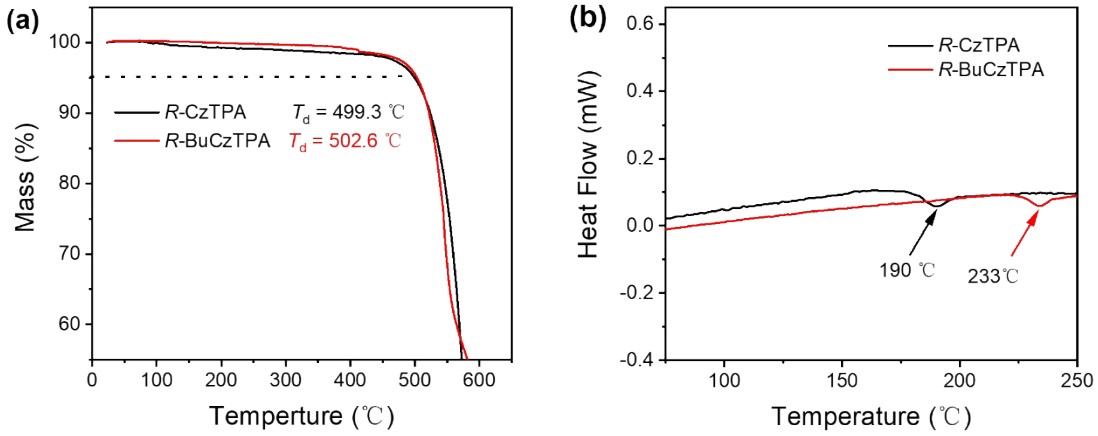

Fig. S1 (a) TGA spectra and (b) DSC spectra of ***R*-CzTPA** and ***R*-BuCzTPA**.

6. Electrochemical Properties

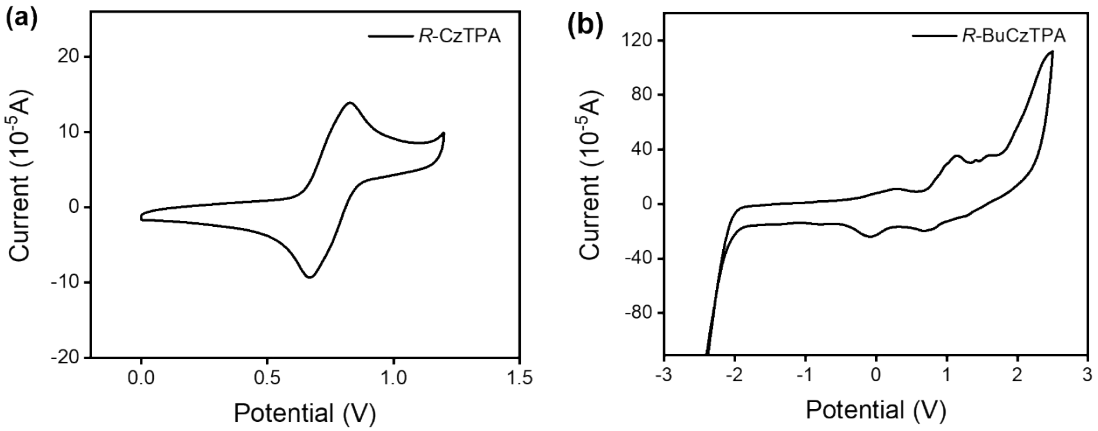

Fig. S2 Cyclic voltammogram curves of (a) ***R*-CzTPA** and (b) ***R*-BuCzTPA** measured in CH_2Cl_2 containing 0.1 M tetra-n-butylammonium hexafluorophosphate.

Tab. S1 Electrochemical properties and theoretical calculations.

Compound	λ_{onset} (nm)	*Eg* [a] (eV)	*Eg* [b] (eV)	$E_{ox,\ onset}$ (eV)	HOMO/LUMO [a] (eV)	HOMO/LUMO [b] (eV)
***R*-CzTPA**	294	4.22	3.72	0.79	- 5.31/- 1.09	- 5.28/- 1.56
***R*-BuCzTPA**	300	4.13	3.63	0.92	- 5.44/- 1.31	- 5.15/- 1.52

[a] Measured in CH_2Cl_2 at room temperature with ferrocene as an internal standard. [b] Obtained from theoretical calculations. $E_g = 1240/\lambda_{onset}$. $E_{HOMO} = -(E_{ox} - E_{(Fc/Fc+)} + 4.8)$ eV, $E_{(Fc/Fc+)} = 0.28$ eV vs Ag/AgCl. $E_{LUMO} = E_{HOMO} + E_g$.

7. Optical Properties

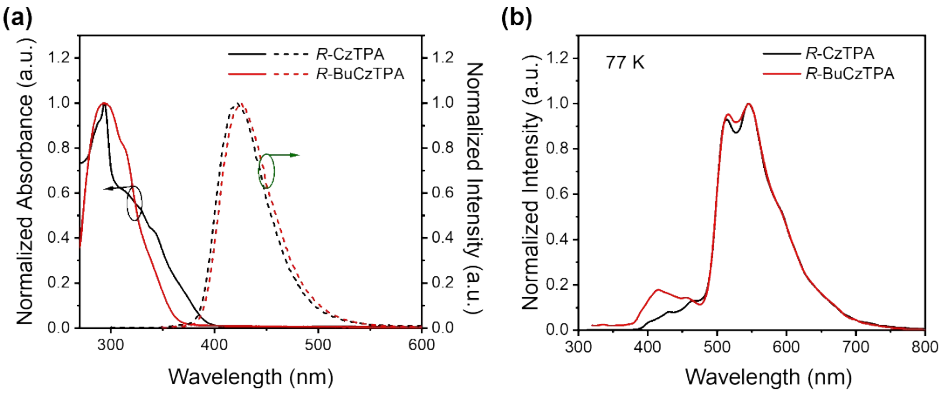

Fig. S3 (a) The UV-Vis absorption (Straight line) and FL spectra (Dash line) of ***R*-CzTPA** and ***R*-BuCzTPA** in toluene (10^{-5} M) at 298 K; (b) the PL spectra of ***R*-CzTPA** and ***R*-BuCzTPA** in toluene (10^{-5} M) at 77 K (λ_{ex} = 290 nm).

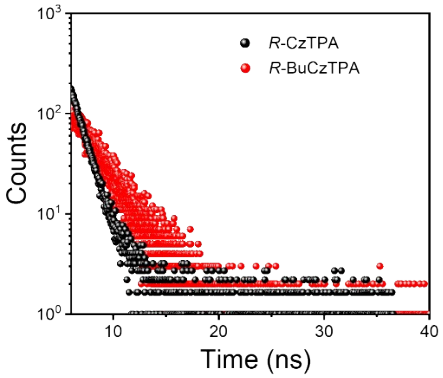

Fig. S4 Fluorescence lifetime curve of ***R*-CzTPA** and ***R*-BuCzTPA** in films at 298 K.

Tab. S2 Photophysical data of ***R/S*-CzTPA** and ***R/S*-BuCzTPA**.

Compound	λ_{ex} (nm)	λ_{em} [a] (nm)	τ_{298K} [b] (ns)	E_T [c] (eV)	$\lvert g_{lum}\rvert$ [a] (10^{-3})	$\lvert g_{lum}\rvert$ [b] (10^{-3})
***R/S*-CzTPA**	290	428	2.7	2.27	5.7	3.6
***R/S*-BuCzTPA**	290	428	2.5	2.27	2.5	1.9

[a] Measured in toluene (10^{-5} M) at 298 K. [b] Measured in neat films. [c] Triplet level.

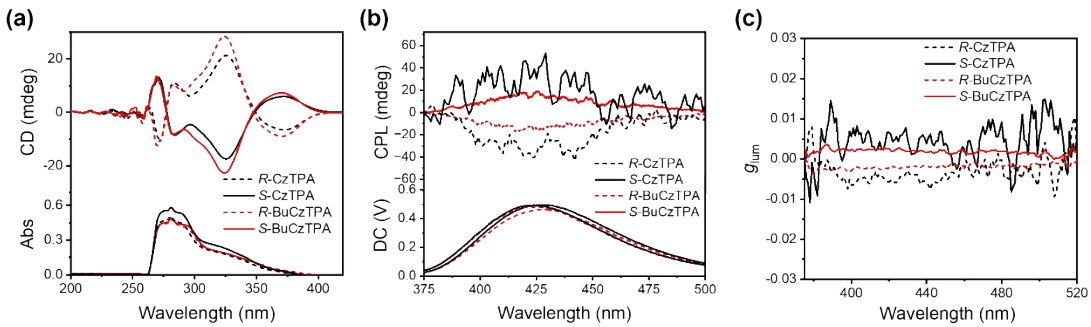

Fig. S5 (a) CD spectra; (b) CPL spectra; (c) g_{lum} versus wavelength curves of ***R/S*-CzTPA** and ***R/S*-BuCzTPA** in toluene (10^{-5} M) (λ_{ex} = 290 nm).

8. Hole-only Devices

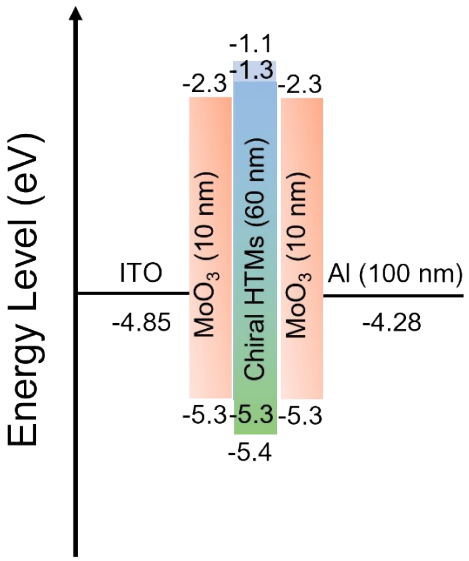

ITO/MoO_3 (10 nm)/Chiral HTMs (60 nm)/MoO_3 (10 nm)/Al (100 nm)

Fig. S6 Device structures of hole-only devices.

9. Measurement of the relative dielectric constant

The relative dielectric constant of chiral hole transport materials by using impedance spectroscopy. According to the definition, impedance Z is expressed as a complex number, as shown below:

$$Z = Z' - jZ'' \tag{1}$$

By substituting the real part Z′ and the imaginary part Z″ of the impedance Z, it can be expressed as:

$$Z' = \frac{R}{1 + (\omega RC)^2} \tag{2}$$

$$Z'' = \frac{\omega R^2 C}{1 + (\omega RC)^2} \tag{3}$$

Where $\omega = 2\pi f$, f is the frequency, C is the capacitance, and R is the resistance. By calculating the modulus of the impedance, we obtain:

$$|Z| = \frac{R}{\sqrt{1 + (\omega RC)^2}} \tag{4}$$

When measuring semiconductor devices, the device formed by the electrode materials typically possesses a geometric capacitance C_g, and in this case, Cg = C. Therefore, the following expression can be obtained:

$$Cg = C = \frac{Z''}{\omega |Z|^2} \tag{5}$$

According to the dielectric–capacitance equation, the following can be obtained:

$$\varepsilon' = \frac{C_g d}{\varepsilon_0 A} \tag{6}$$

$\varepsilon_0$is the vacuum permittivity, *d* is the thickness of the dielectric layer, and *A* is the area of the dielectric. The value of ε_0 is 8.854 × 10^{-12} A^2 s^4 kg^{-1} m^{-3}. By substituting Equation (6) into the capacitance–dielectric relation, the real part of the dielectric constant ε′ (i.e., the commonly used relative dielectric constant) can be expressed as:

$$\varepsilon' = \frac{C_g d}{\varepsilon_0 A} = \frac{d}{\varepsilon_0 A} \cdot \frac{Z''}{\omega |z|^2} \tag{7}$$

By substituting Equation (7), the dielectric constants were calculated as follows: ε_{CzTPA} = 2.8, $\varepsilon_{BuCzTPA}$ = 4.6.

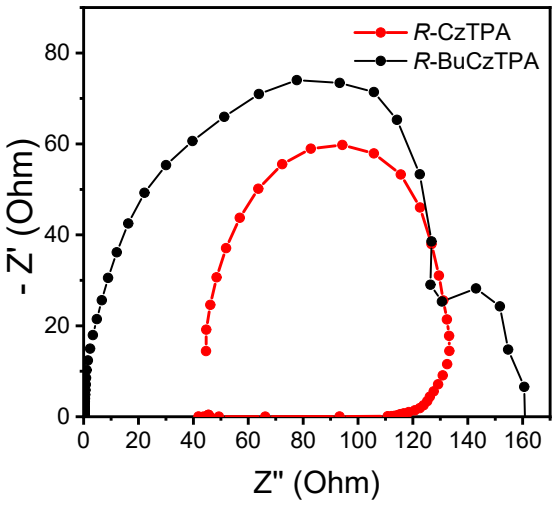

Fig. S7 Impedance spectra of the chiral hole transport materials.

10. Electroluminescence Properties

Tab. S3 CP-OLEDs data of ***R/S*-CzTPA** and ***R/S*-BuCzTPA**.

Device	V_{on} [a] (V)	L_{max} (cd m^{-2})	λ_{EL} [b] (nm)	CE_{max} (cd A^{-1})	EQE_{max} (%)	g_{EL} (10^{-3})
***R*-A**	4.5	42859	508	16	5	- 0.89
***S*-A**	4.0	34816	508	17	5	+ 0.85
***R*-B**	3.0	94449	508	62	19	- 1.20
***S*-B**	3.0	93661	508	61	18	+ 1.60
***R*-C**	4.5	24658	504	23	7	/
***S*-C**	3.5	33168	504	23	7	/
***R*-D**	3.0	34555	508	35	10	- 0.57
***S*-D**	3.5	42494	508	33	10	+ 0.54

[a] Turn on voltage recorded at a brightness of 1 cd m^{-2}. [b] Electroluminescence peak at 11 V.

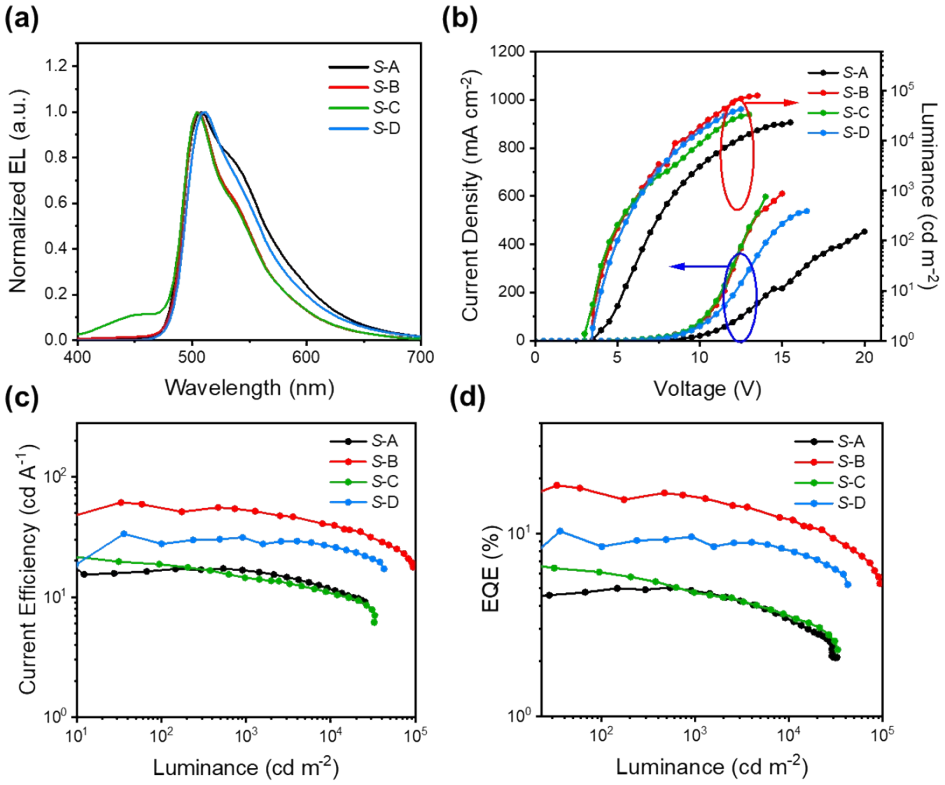

Fig. S8 Device performance for *S*-A/B/C/D. (a) EL spectra; (b) current density-voltage-luminance (*J*-*V*-*L*) characteristics; (c) current efficiency-luminance curves; (d) external quantum efficiency-luminance curves.

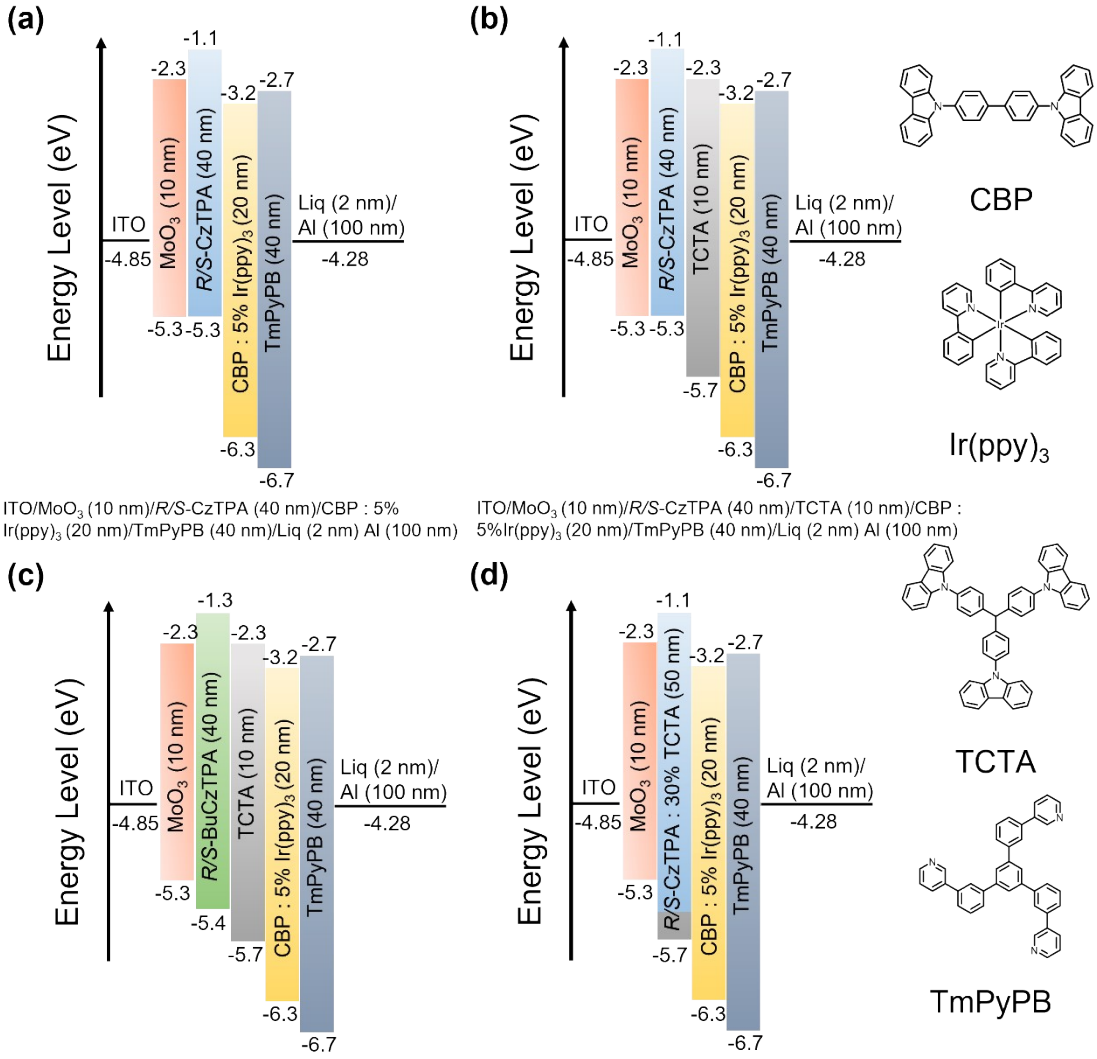

Fig. S9 Device structures of *R/S*-A/B/C/D (The illustration shows the molecular structures used in OLEDs).

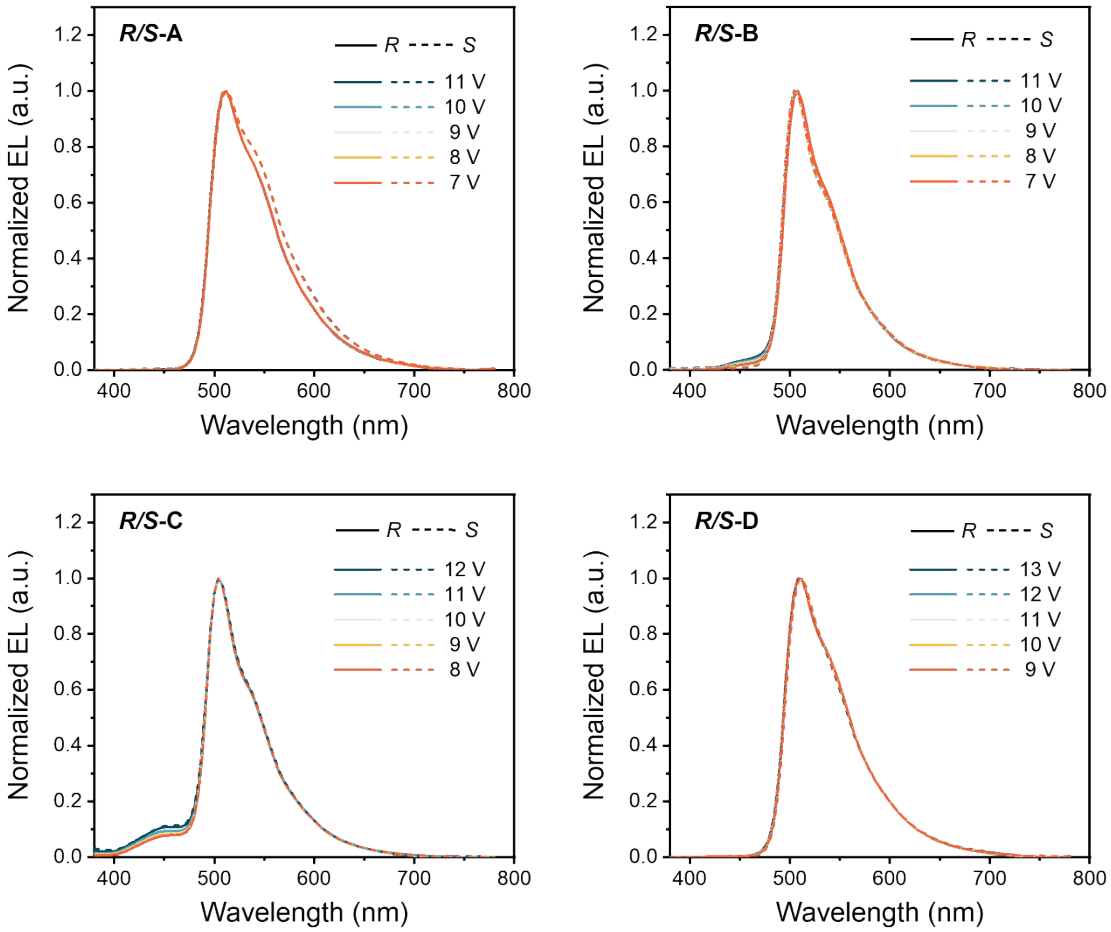

Fig. S10 EL spectra of devices *R*/*S*-A/B/C/D at different voltages.

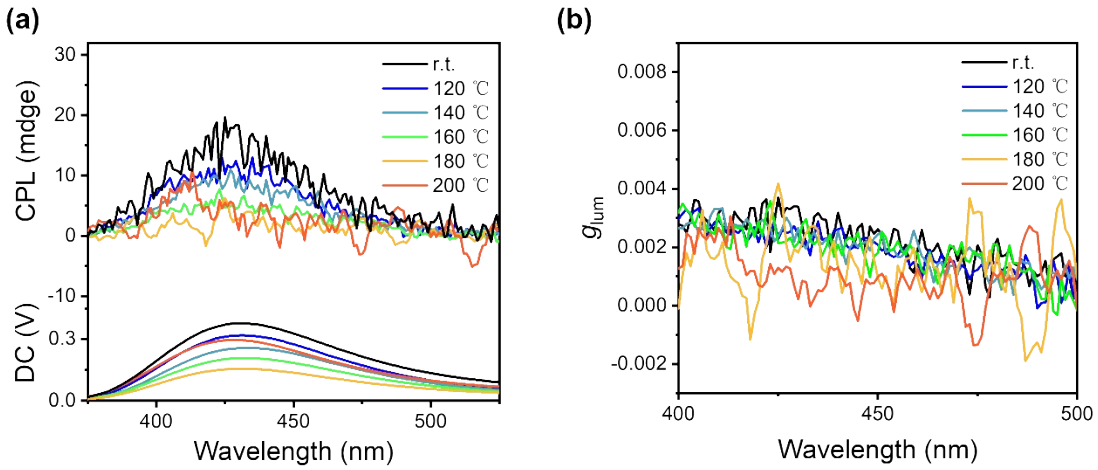

Fig. S11 CPL spectra of ***S*-CzTPA** films after thermal annealing at different temperature (λ_{ex} = 290 nm).

Tab. S4 g_{lum} values of ***S*-CzTPA** films after thermal annealing at different temperature.

Annealing Temperature (℃)	g_{lum} (10^{-3})
r.t.	+ 3.4
120	+ 3.3
140	+ 3.0
160	+ 3.0
180	+ 1.8
200	+ 0.2

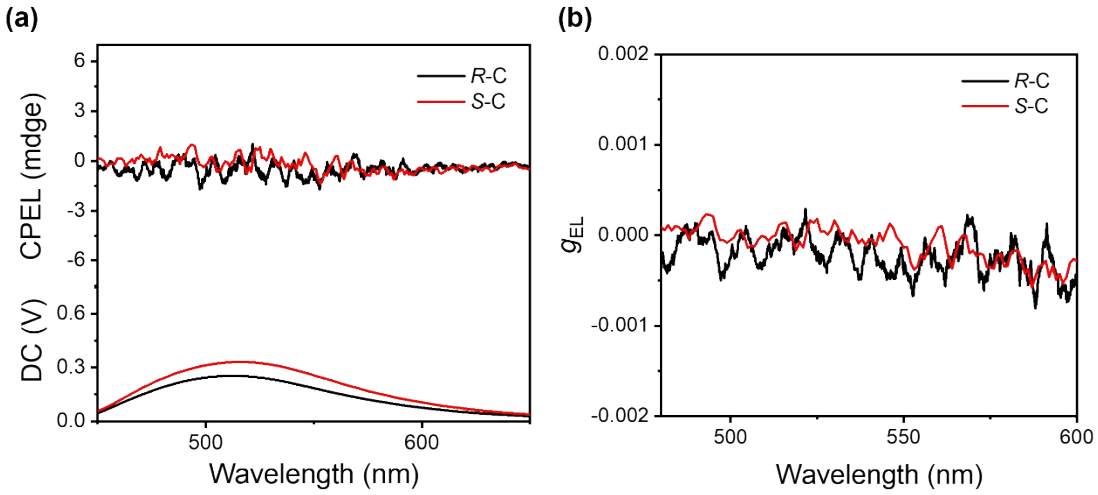

Fig. S12 (a) CP-EL spectra and (b) g_{EL} value spectra of devices *R*/*S*-C.

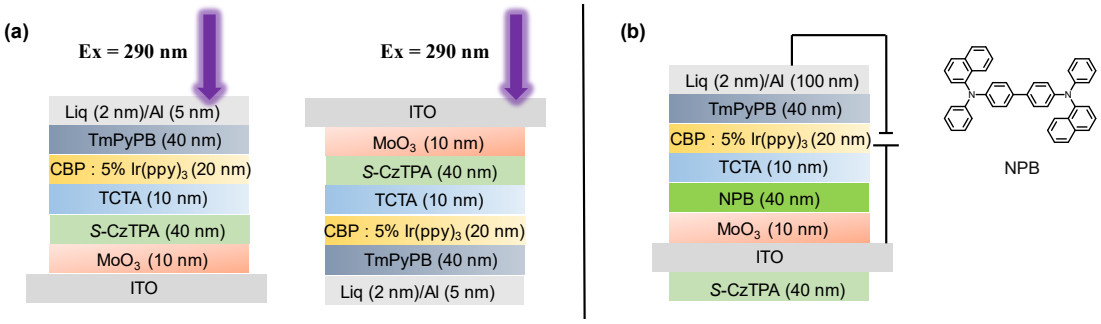

Fig. S13 Device structures of (a) E (b) F.

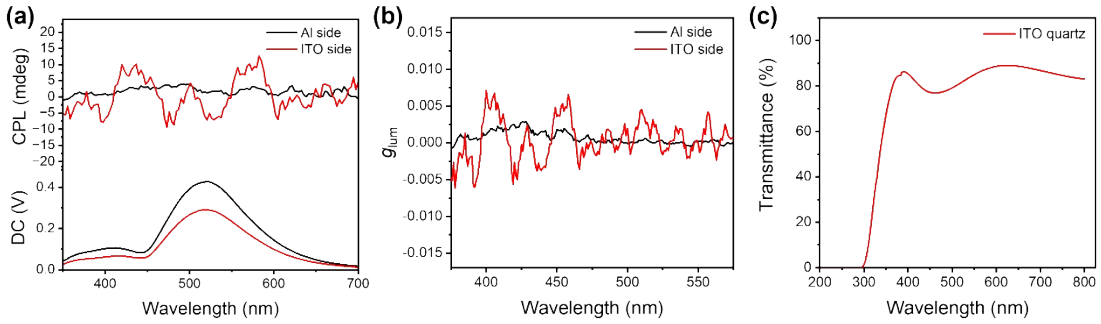

Fig. S14 (a) CPL spectra and (b) g_{lum} value of device E; (c) transmittance spectrum of ITO glass substrate.

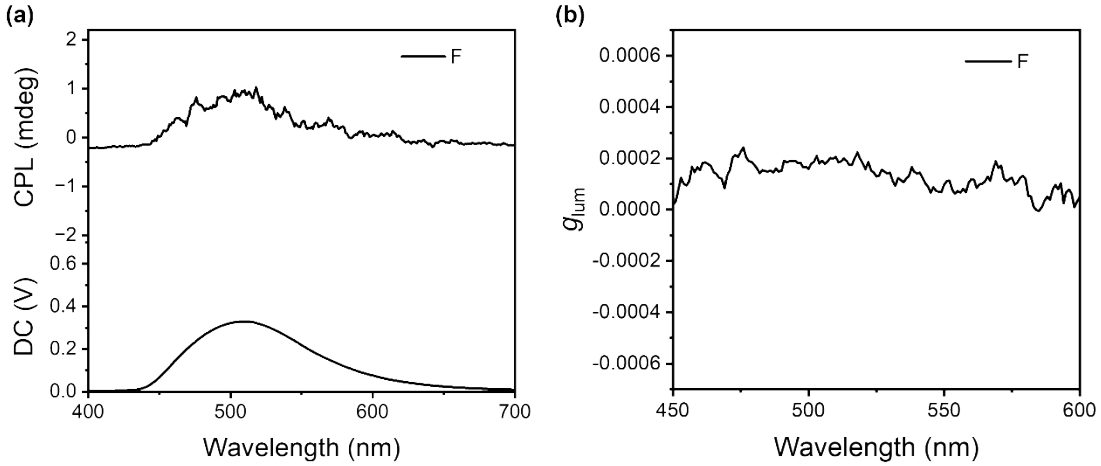

Fig. S15 (a) CPL spectrum and (b) g_{lum} value of device F.

11. NMR Data

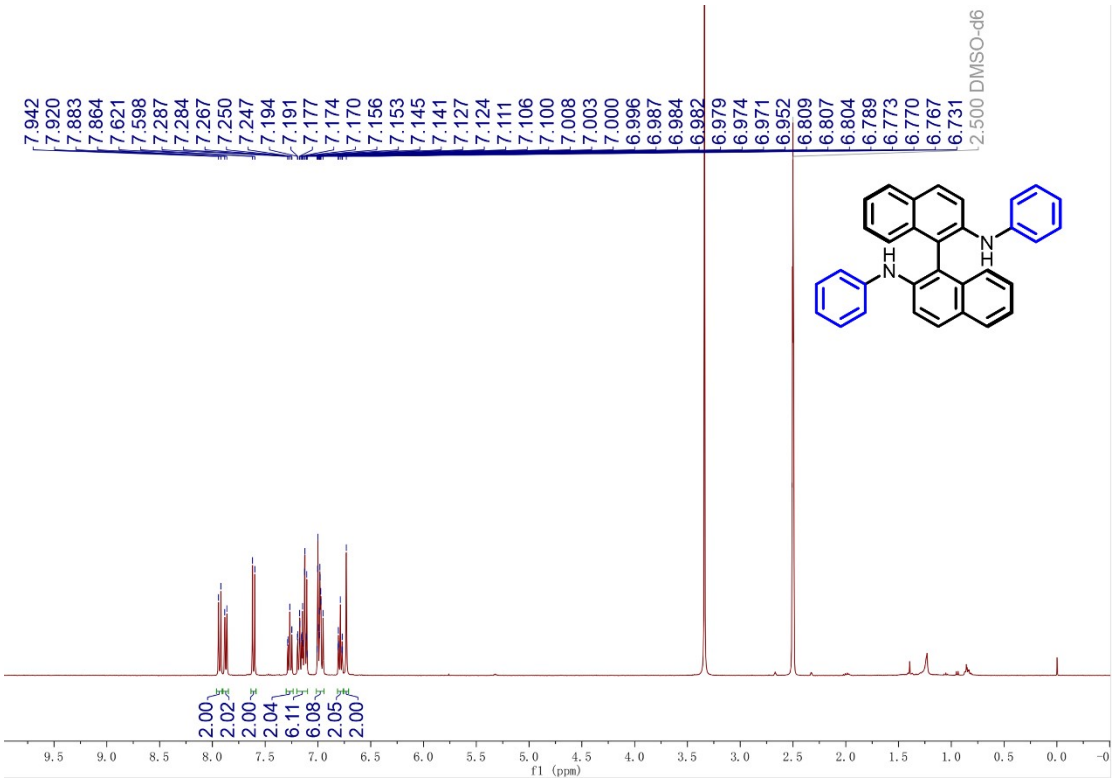

Fig. S16 ^{1}H NMR spectrum of ***R*-TPA** in DMSO-*d6*.

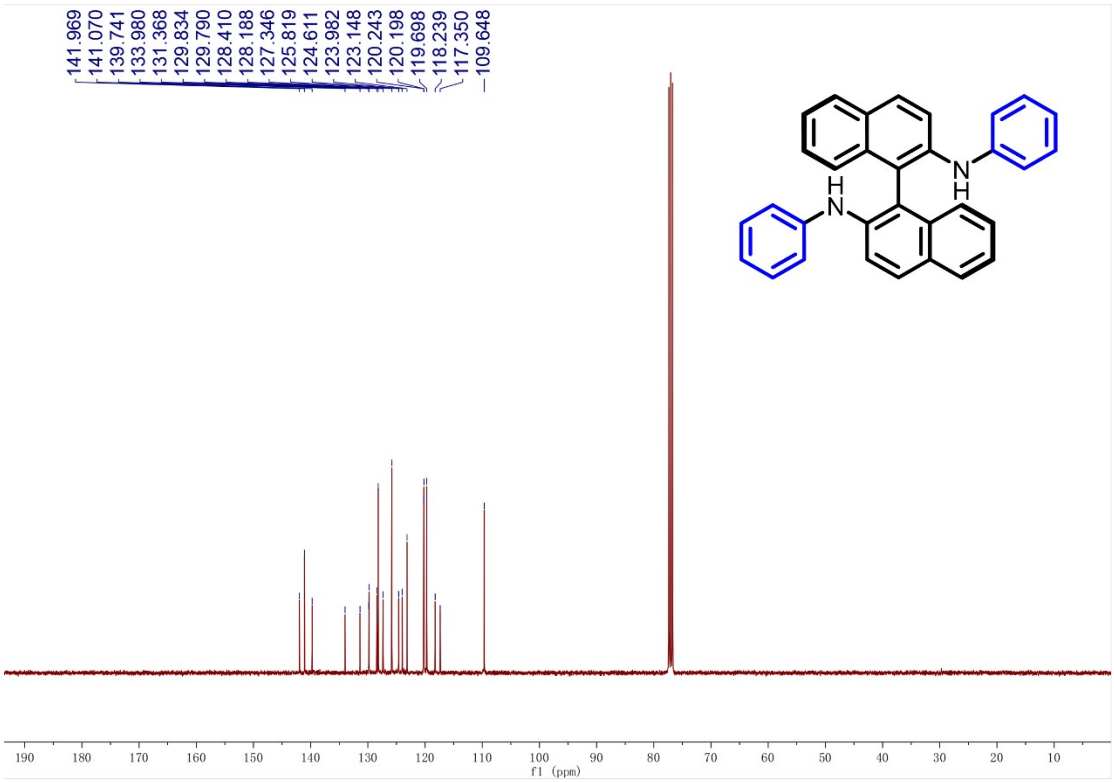

Fig. S17 ^{13}C NMR spectrum of ***R*-TPA** in $CDCl_3$.

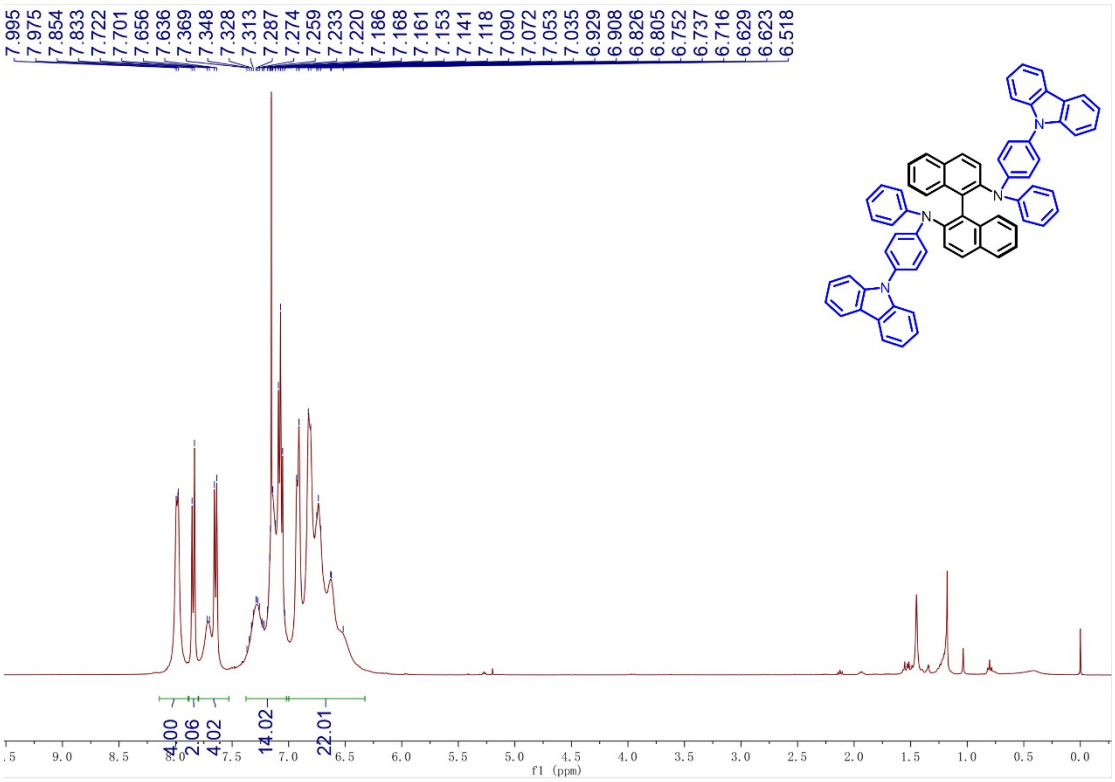

Fig. S18 ^{1}H NMR spectrum of ***R*-CzTPA** in $CDCl_3$.

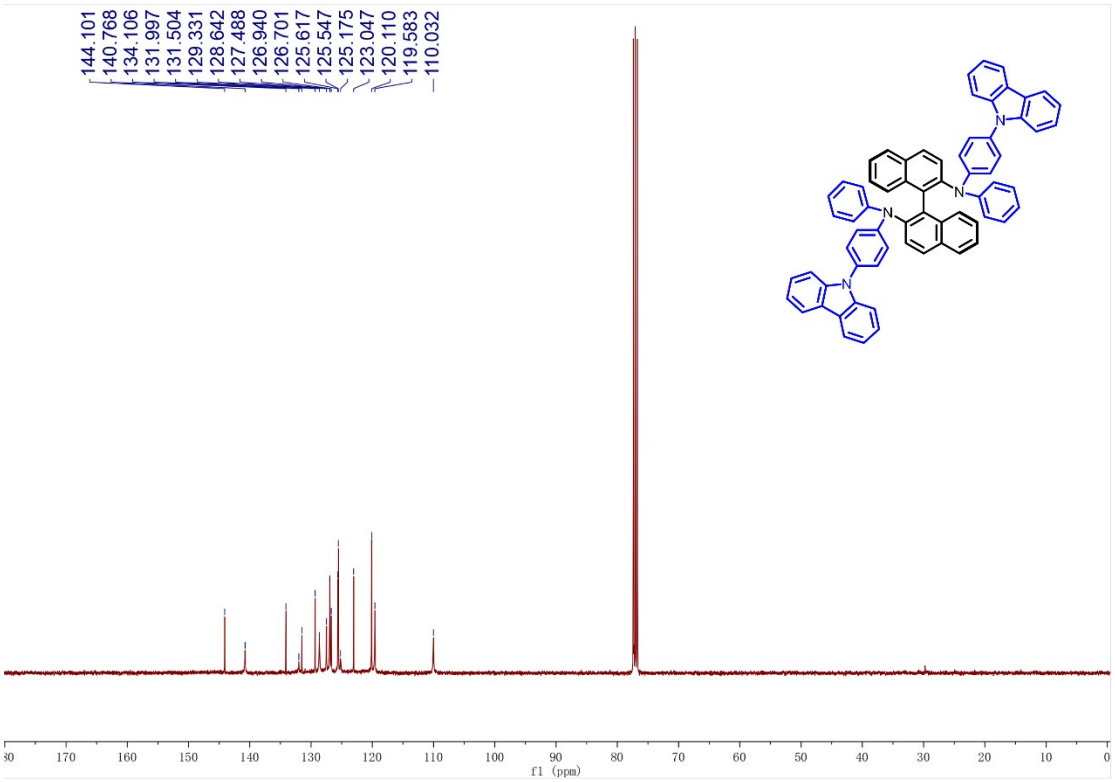

Fig. S19 ^{13}C NMR spectrum of ***R*-CzTPA** in $CDCl_3$.

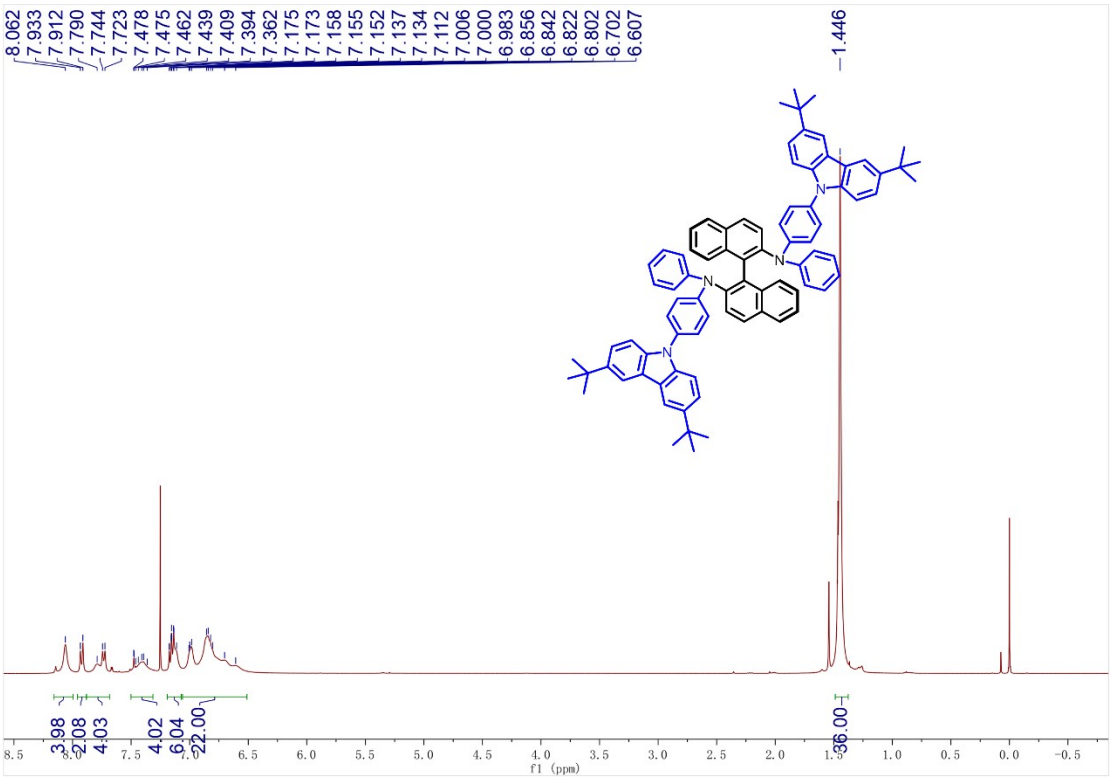

Fig. S20 ^{1}H NMR spectrum of ***R*-BuCzTPA** in $CDCl_3$.

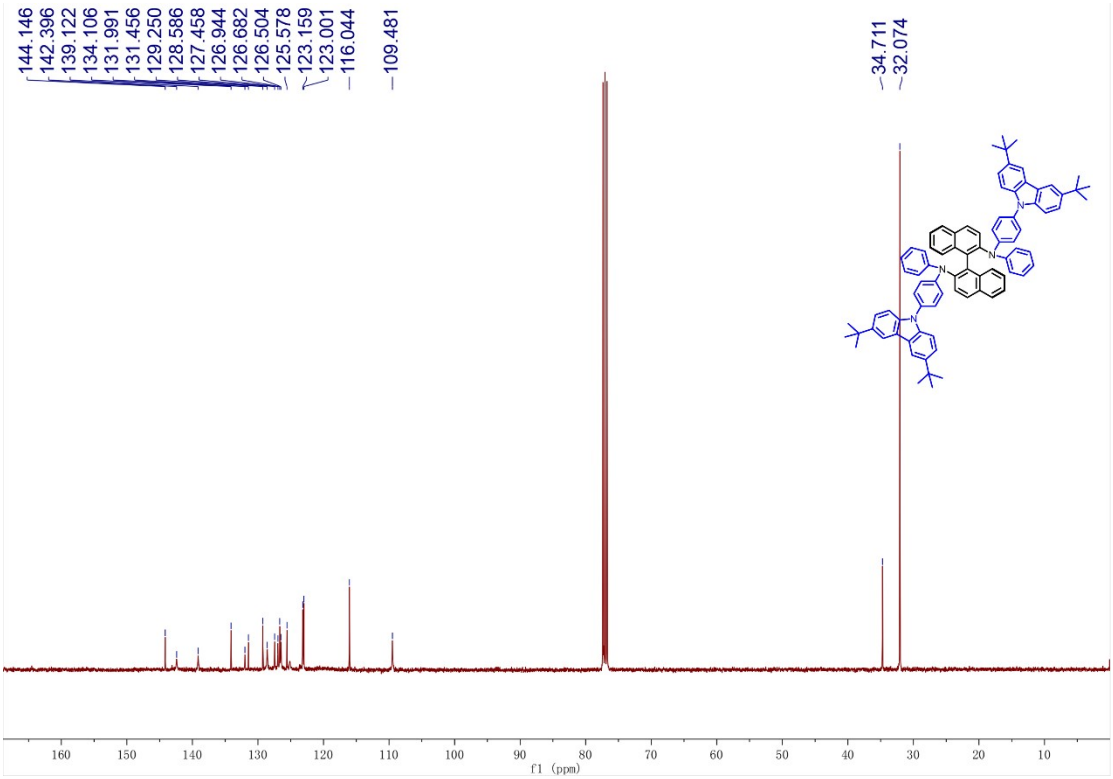

Fig. S21 ^{13}C NMR spectrum of ***R*-BuCzTPA** in $CDCl_3$.